Waikiki Camera Analysis

United States Army Corps of Engineers, Honolulu Engineering District
EA/HHF Joint Venture
University of Hawaii at Manoa, School of Ocean and Earth Science and Technology

US Army Corps of Engineers ®

EA/HHF Joint Venture

SCHOOL OF OCEAN AND EARTH SCIENCE AND TECHNOLOGY

Introduction

The interaction between nearshore hydrodynamics and beach sedimentation is reflected in the morphodynamic response of the beach. Theory on sediment transport is used to formulate the interactive processes, but the level of uncertainty manufactured in field applications reveals that the theory is in a premature state. As a result, methods based on empirical studies are often used to quantify local interactions between forcing parameters and beach response.

Observations of surf parameters and beach dynamics aid coastal management around the world. The U.S. Army Corps Regional Sediment Management program is interested in improving management of sediment in the Hawaii coastal zone. On Oahu, Hawaii, studies have identified features within individual littoral cells (Moberly and Chamberlain, 1964; Campbell, 1972; Gerritsen, 1978; Gibbs et al., 2001). Within the past decade, advances in observing beach processes have been made using high resolution techniques (Dail et al., 2000; Norcross et al., 2002). While seasonal and annual interactions have been resolved to a large extent, interactions on the scale of wave events have yet to be fully resolved.

The use of video imagery significantly improves both the spatial and temporal scales used to quantitatively measure beach response (Holland, K. et al. 1997). Capable of operating as an autonomous remote system, spatial and temporal measurements can be made on scales as fine as centimeters and seconds respectively. Used in conjunction with numerical models, the link between forcing parameters and beach response can be examined at high resolution. Conducting a detailed analysis at these scales helps reduce the level of uncertainty in the development of coastal engineering projects and improves environmental awareness of the effects both down drift and up drift of the site location.

The objectives of the present study are; 1) analyze video imagery data taken from the roof top of a high building located on Waikiki beach on the island of Oahu, Hawaii and quantify the beach response over the course of approximately one and a half years; 2) use local hydrodynamic observations in order to examine the interactions between forcing parameters and beach response.

Environmental Setting

Located in the middle of the North Pacific Ocean, the islands of Hawaii are subjected to a diverse wave climate consisting of both swell and wind waves. The swell environment is seasonal and spatially dependent. Focusing on the south shore of Oahu (Fig. 1), storms in the south Pacific generate long period waves that propagate north during the summer season creating a relatively high energy wave climate. During the winter season, wave energy is relatively low. Superimposed on swell events, wind waves generated by northeast trade winds are most apparent during the summer season, but exist throughout much of the year. During the winter season, local Kona storms induce high energy waves on west and south facing shorelines, but may also occur year-round. Although infrequent, the combined high energy – short period waves carry the potential to cause extensive damage.

This research was performed and the document written by Troy Heitman, Department of Ocean Resources Engineering, SOEST, UH

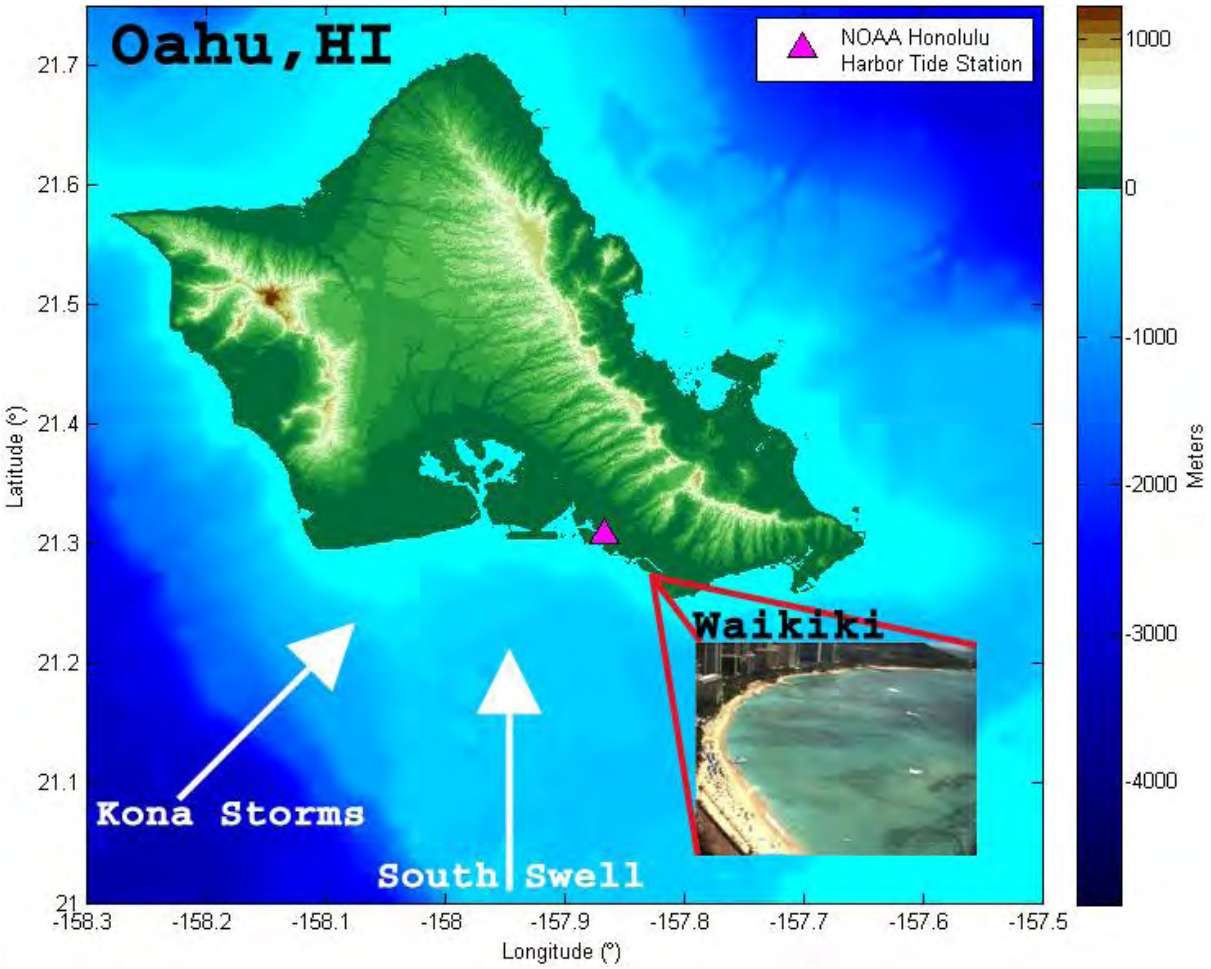

Figure 1 Map of Oahu, HI identifying location of NOAA tide station and south shore wave climate. Location of study is shown with an aerial video image of Waikiki Beach taken from roof top of the Sheraton Waikiki Hotel.

The coast of Oahu is divided into littoral cells defined by topographic and bathymetric barriers to sediment transport, circulation, and wave energy. Natural headlands, submerged sand channels, fringing reefs, and steep slopes are among the most common defining features. The beaches are predominantly made up of calcareous sediment derived from biological activity on adjacent reefs. While Waikiki beach is arguably one of the world's most famous beaches, ironically, it is characterized as being largely manmade. Composed of a series of groins, jetties, seawalls, and sand nourishment projects, the beach requires costly maintenance. Analyzing Waikiki beach processes may help reduce maintenance costs and improve management.

Methodology

Shoreline Identification

A remotely operated video camera is mounted on top of the Sheraton Waikiki hotel. It is oriented to view a segment of the Waikiki shoreline as shown in Figure 1. Digital images were acquired daily between noon and 1pm every 10 minutes from

September 24, 2008 to April 22, 2010. Oriented in the perspective of the camera, the resulting image time series was transferred to a 3-D geographic frame of reference using a semi-implicit photogrammetric transformation method solving the following colinearity equations:

$$u = \frac{L_1 x + L_2 y + L_3 z + L_4}{L_9 x + L_{10} y + L_{11} z + 1}$$

$$v = \frac{L_1 x + L_2 y + L_3 z + L_4}{L_9 x + L_{10} y + L_{11} z + 1} \quad (1)$$

where u and v are image coordinates; x y z are geographic coordinates; and $L_{1...11}$ are direct linear transform (DLT) coefficients (Holland, K. et al. 1997). To solve equation (1), ground control points (GCP) defined within the field of view at known static locations are utilized. The three points (A, B, C) shown in Figure 2 are located on coastal groins and concrete structures. Using light detection and ranging (LiDAR) data, the geographic location of these points is known.

Knowing both the camera and geographic coordinates of the GCP, the only remaining variables to solve are the DLT coefficients. Based on the camera properties and orientation, the DLT coefficients were solved using a semi-implicit nonlinear regression fit.

With a focus on beach response, a region within the image was isolated for analysis. Pixels that fall within the defined region are then transferred to geographic coordinates using equation (1) as shown in Figure 3. The transformation assumes a constant z-reference leaving 2 equations and 2 unknowns, x and y, and equation (1) is solved explicitly.

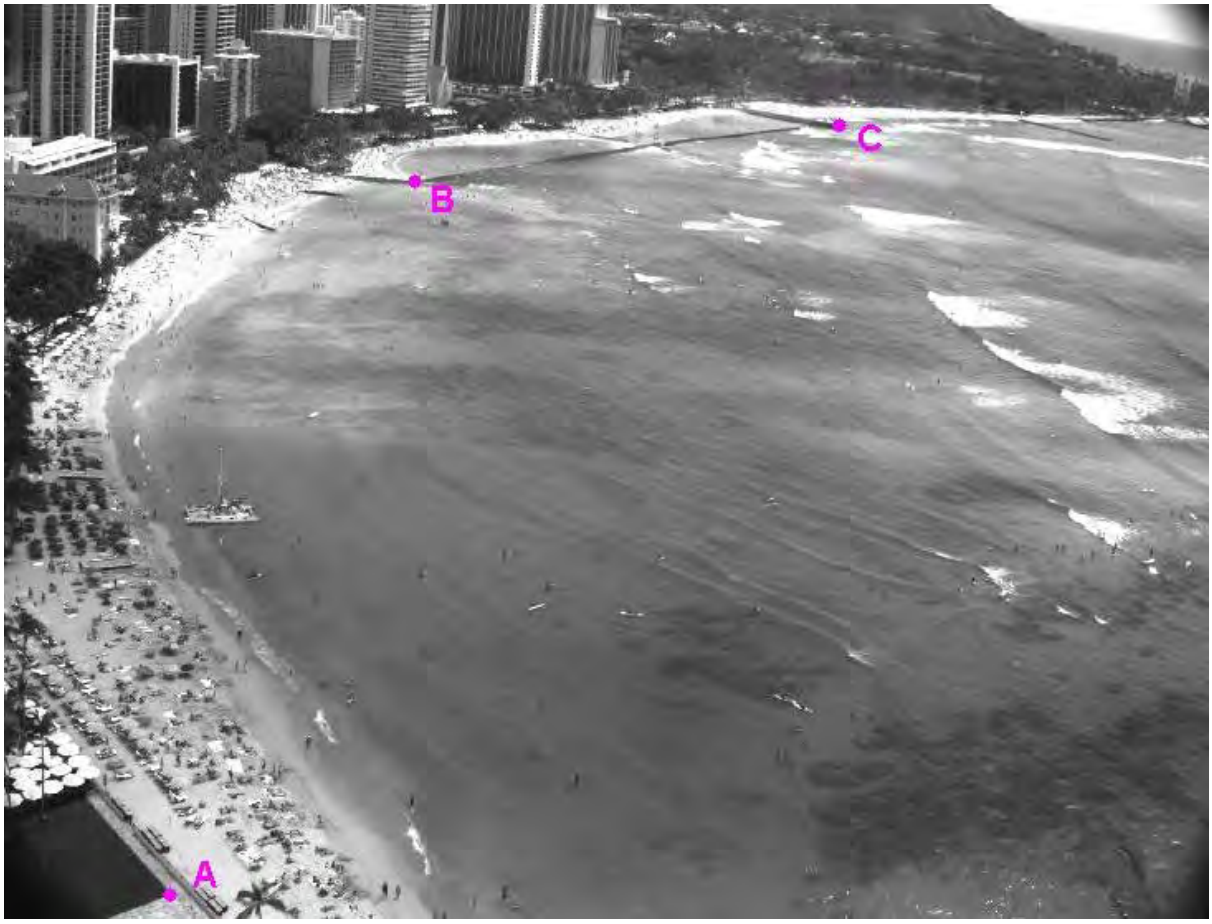

Figure 2 Location of ground control points (GCP)

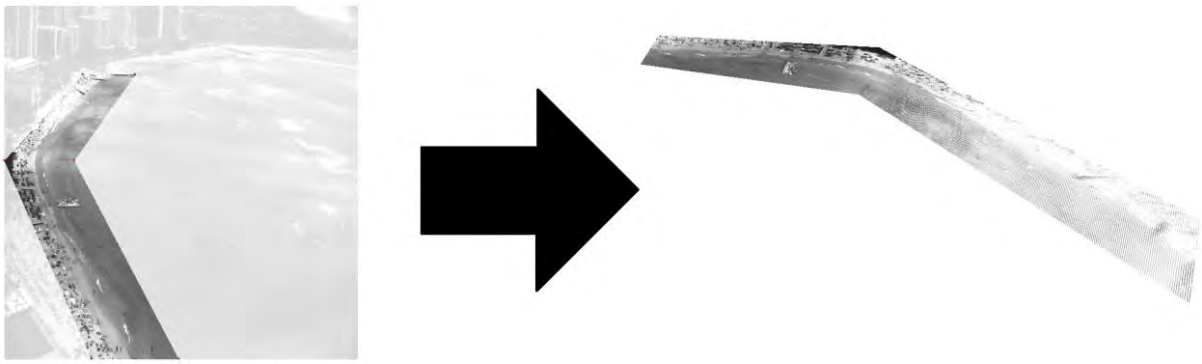

Figure 3 Transformation from camera to geographic coordinates. Transects shown on geographic reference image.

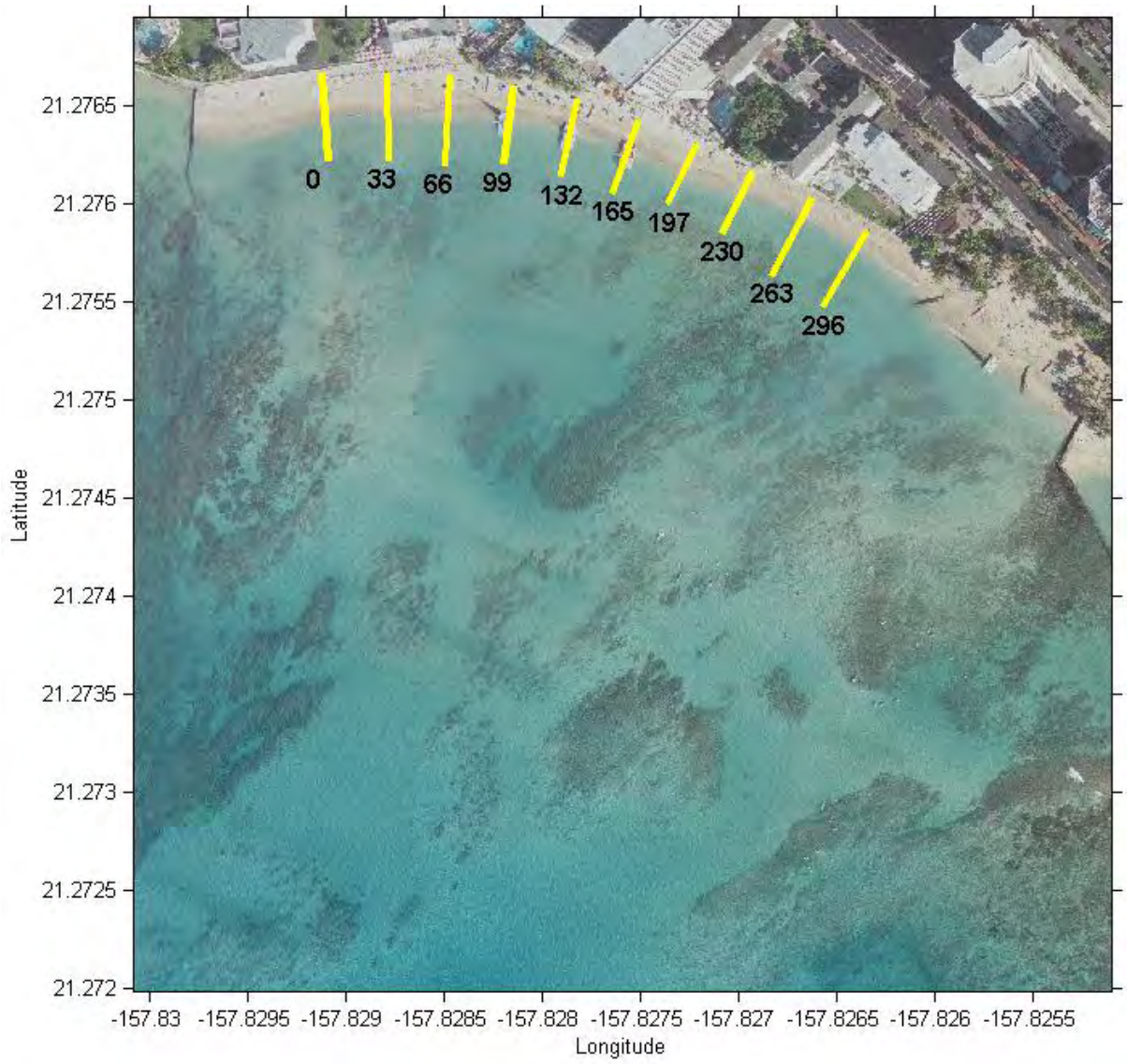

Figure 4 Transect locations on geographic reference image. Approximate spacing between transects is identified in yards.

The transformation allows transects to be drawn orthogonal to the shoreline defining a principle axis with cross-shore and alongshore coordinates. Figure 4 shows 10 transects that are spaced approximately 33 yd apart. At each transect, pixels were interpolated to create a 1-D cross-shore image. Extracted from each image in the time series, the 1-D cross-shore images were compiled to produce a time-series revealing the changing character of the shoreline at each transect. Figure 5 shows a time stack of 1-D cross-shore images for the first (western) transect. The Y axis depicts the cross-shore direction and is oriented such that the bluish color along the bottom is the ocean, while the brownish color is the beach. The X axis represents time. The black bars indicate periods when the camera was inoperable.

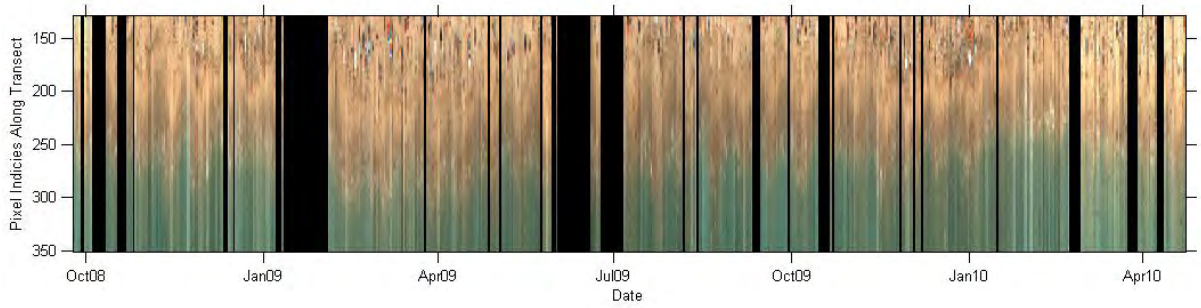

Figure 5 Time series of cross-shore shoreline positions for transect 1

The shoreline in this time series is defined using a method that measures color channel divergence (CCD) between red, green, and blue (RGB) color channels (Turner, I. et al. 2001). The method is based on the principle that water does not reflect red light as well as the beach, thus the red component of the RGB channel captured by the camera will diverge rapidly at the land-sea interface. Figure 6 shows the application of the CCD method used to define the shoreline position on day 1 of the first transect. The high frequency oscillations in each RGB channel are filtered using a low-pass filter and the shoreline position is objectively defined by the furthest offshore point of intersection between the red and green filtered channels. The shoreline is identified at a pixel index value of approximately 235.

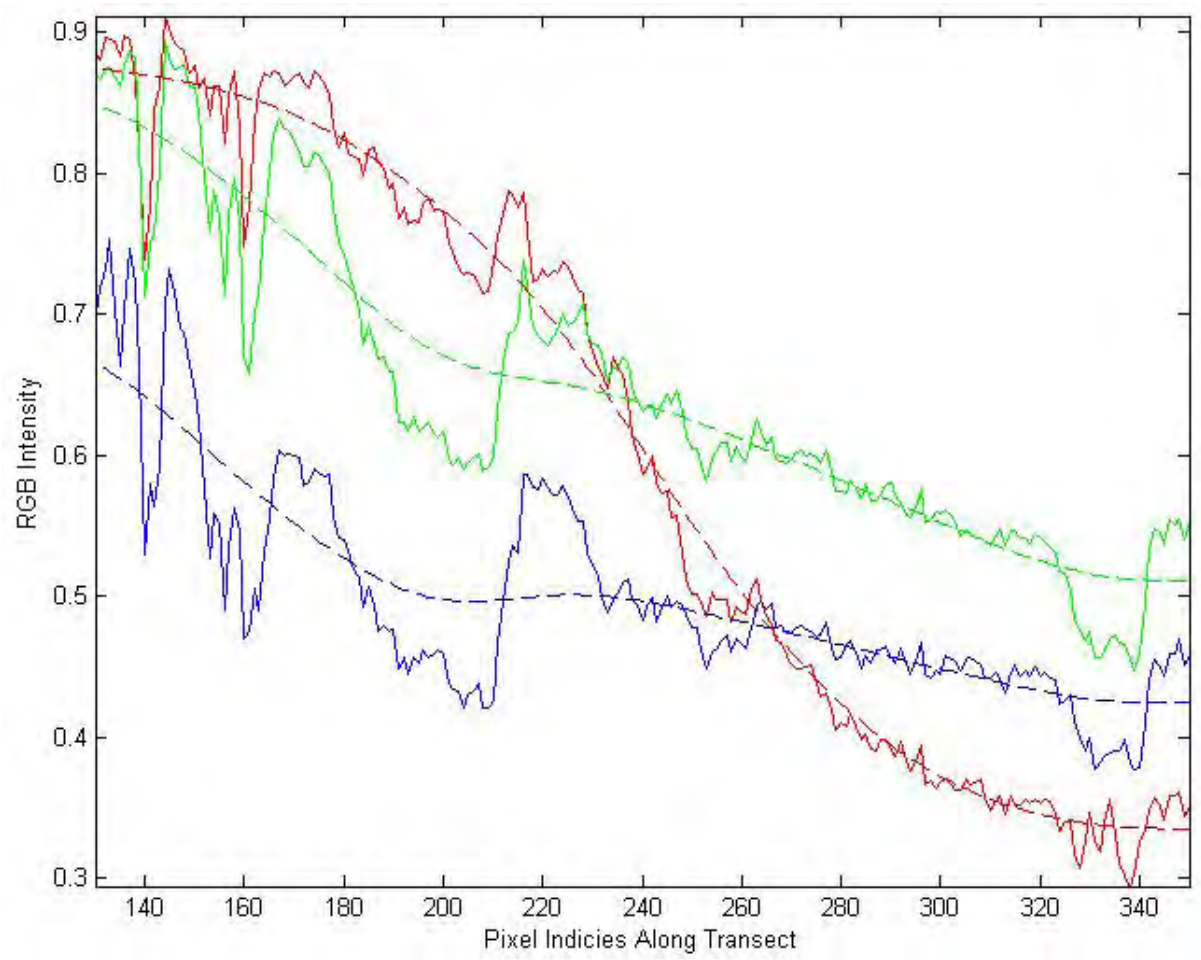

Figure 6 Application of CCD method to identify shoreline position

Beach traffic on Waikiki presents the potential for erroneous identifications of shoreline position. To filter out any such occurrences, binary values were assigned to each pixel based on the identified shoreline position. Locations landward of the shoreline received a value of 1, while locations seaward received a value of 0. The resulting binary image was then cleaned using logical filtering techniques. Figure 7 shows the unfiltered binary image and resulting shoreline position identified for transect one. Zooming in on a section of the identified shoreline position reveals the effectiveness of the method.

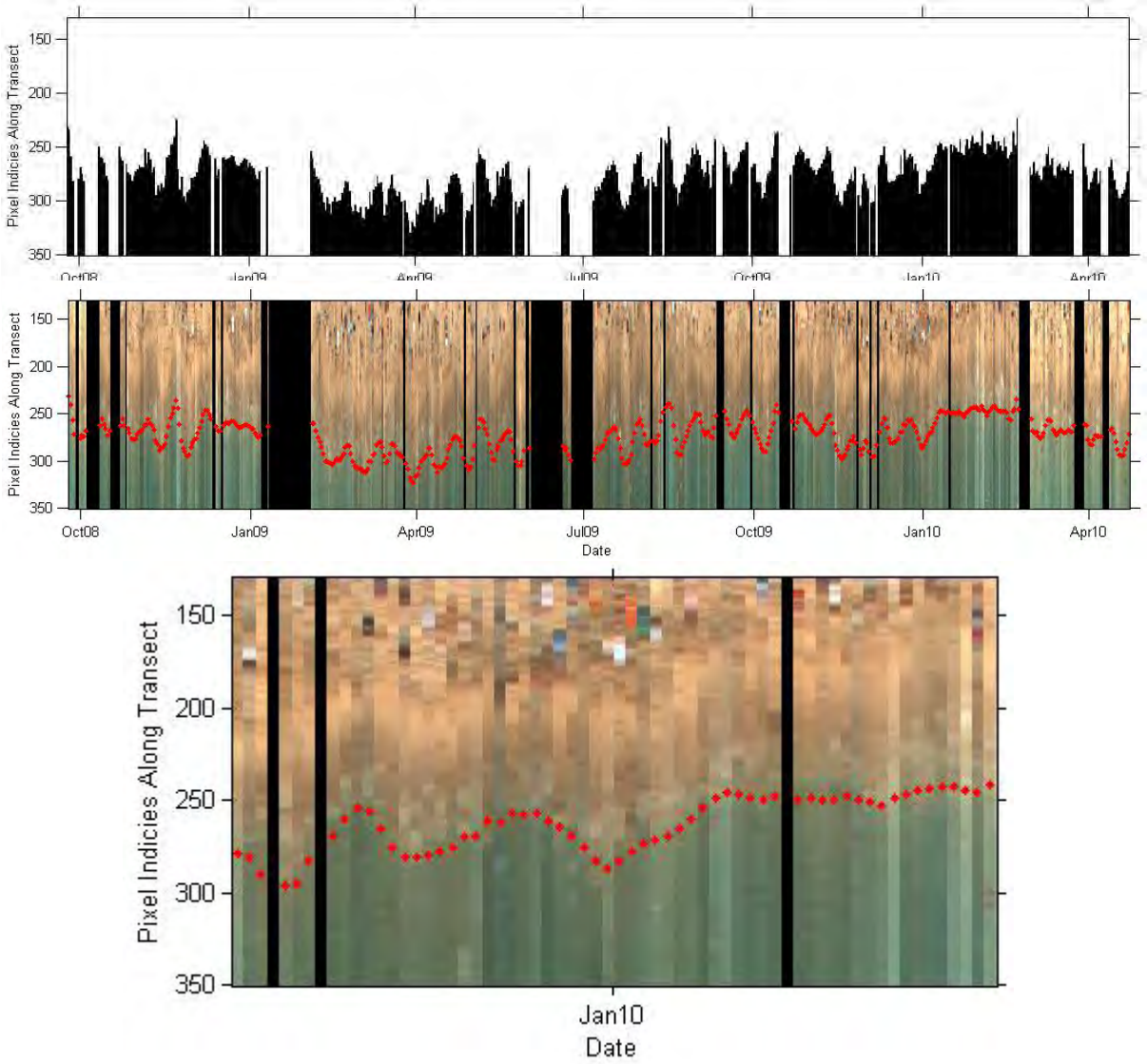

Figure 7 Top: Unfiltered binary image of shoreline position. **Middle**: Filtered shoreline position. **Bottom**: Zoom of filtered shoreline position.

For each transect, the shoreline position identified on day 1 is used as a reference to measure the relative change in shoreline position over the course of the study. The result shown in Figure 8 is a 2-D representation of the beach response relative to the

reference. Distances measured onshore of the reference are chosen as positive (red), while distances measured offshore are negative (blue). The alongshore component is measured from west to east (0-295 yd) and interpolated to a resolution of 5.46 yd. The cross-shore component is represented with a color bar depicting relative shoreline position. The plot on the right of Figure 8 shows the application of a linear regression through time (X axis) as a function of the alongshore direction (Y axis). The onshore-offshore frame of reference implies that negative change rates signal accretion while positive change rates signal erosion.

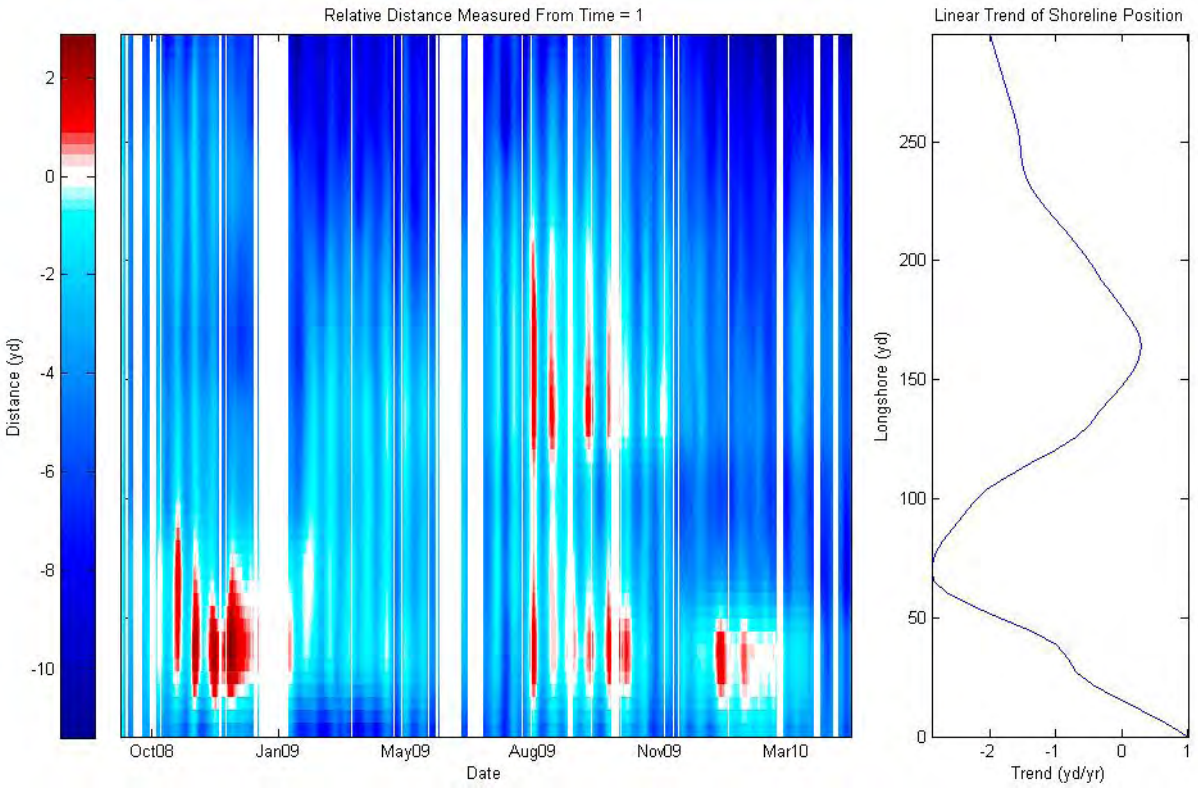

Figure 8 Left: 2-D temporal beach response relative to first identified shoreline position. **Right**: Linear trend of shoreline position as a function of longshore direction.

Wave Parameters

The nearby Kilo Nalu ocean observatory, managed by the University of Hawaii Ocean and Resources Engineering Department, is used as a resource to obtain local wave data. Observations are made on a depth contour of approximately 40ft. Despite being located a few miles away, observations of significant wave height and peak period provide sufficient offshore conditions. The mean wave direction should be used with caution as the effects of refraction are present. A significant amount of wave data is missing throughout the summer season resulting in a winter season biased. Figure 9 shows the distributions of wave parameters experienced over the course of the study period.

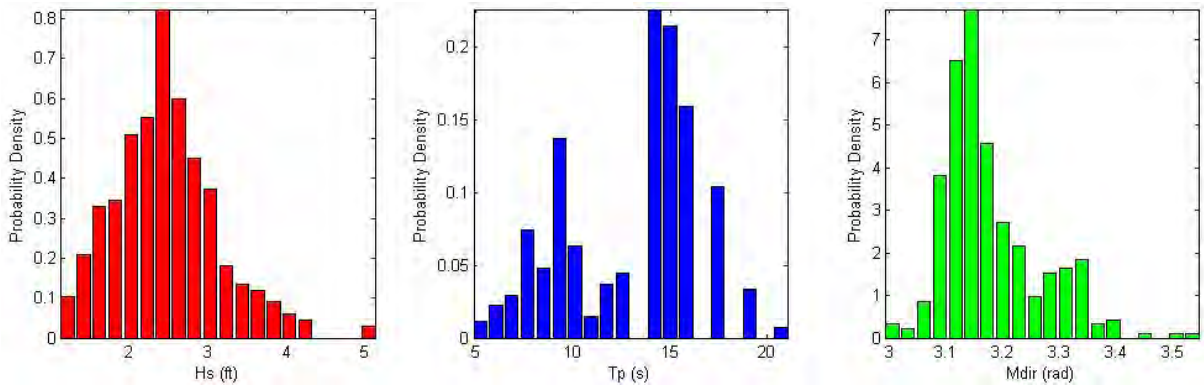

Figure 9 Probability density of wave observation over course of study

Tidal Influence

The shoreline position is a reflection of local water levels governed by environmental forcing parameters. Therefore, the shoreline position alone does not indicate beach erosion or accretion. The temporal variability of the shoreline position can be purely the result of fluctuating water levels. To decompose the shoreline position, a water level model described by Aarninkhof et al., 2003 is used

$$Z_{sl} = Z_{tide} + \eta_{sl} + k_{osc} \cdot \frac{\eta_{osc}}{2} \qquad (2)$$

where Z_{tide} is the local tide elevation, η_{sl} is the wave setup at the shoreline, η_{osc} is the rms swash height, and k_{osc} is a tuning coefficient. The contributions of wave setup and swash height are dependent on wave conditions, therefore are functions of both time and space. Over the course of the study period, the availability of incident wave data is temporally limited. The study area is also composed of both sand channels and fringing reefs, as shown in Figure 4. This introduces spatial variability in the calculated wave energy and momentum at the beach face due to the differences in geological control on the wave field (Gourlay, 1996). The current study uses an hourly average of the shoreline position and assumes the effects of wave setup and swash height are minimized, reducing equation (2) to a function of tide only.

Verified tides were taken from the Honolulu Harbor tide station operated by NOAA shown in Figure 1. Tidal elevations were interpolated to account for the 15 minute phase lag between Waikiki and the tide station (Wang and Gerritsen, 1995). To convert the tidal elevations to a horizontal frame of reference, a beach slope of 1:10 is assumed. The assumption is considered feasible based on nearby profiles surveyed by the University of Hawaii Coastal Geology Group. The time series of tidal variability is shown in Figure 10.

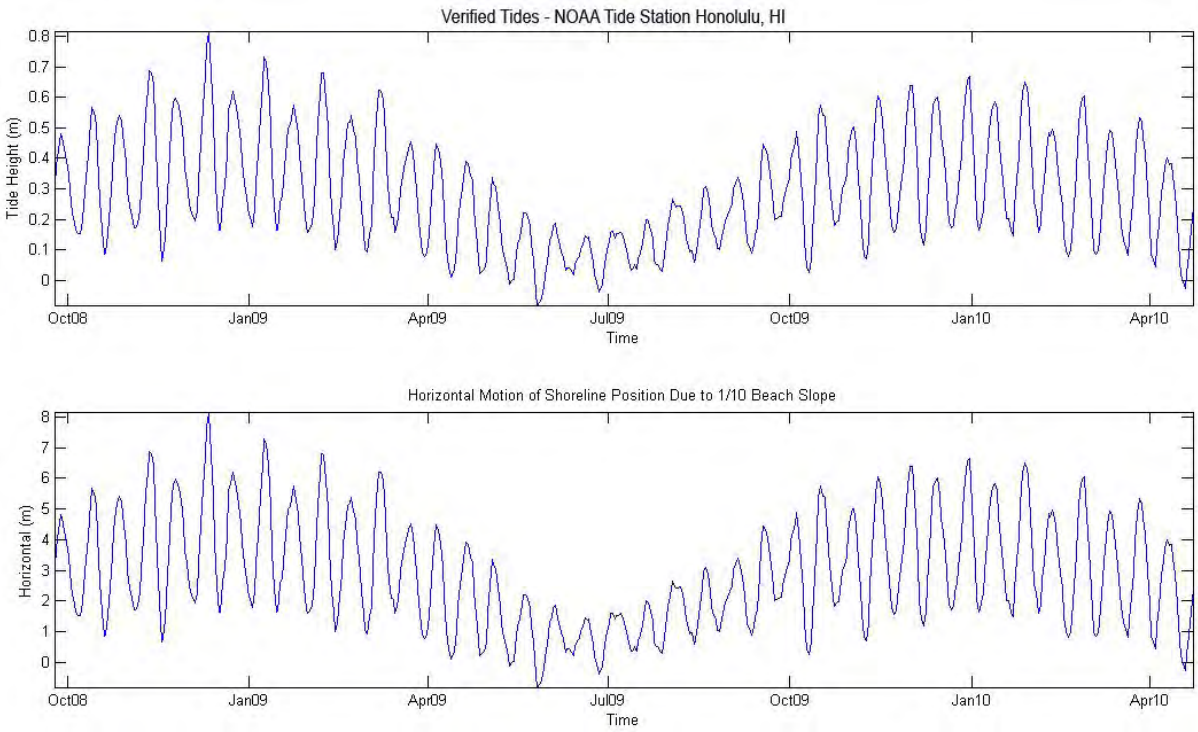

Figure 10 Top: NOAA verified tidal elevations, phase corrected for Waikiki. **Bottom**: Horizontal transformation due to assumption of 1:10 beach slope.

The horizontal contribution of tidal variability can be compared with the time series of shoreline position by assuming that on day 1, the amplitude of the horizontal tide motion defines the shoreline position. The reference point for the horizontal tide time series and shoreline time series is now the same. The dependency of the shoreline position on the tidal variability is shown in Figure 11, where both time series are similar in both phase and amplitude. The linear regression of the shoreline position shown in Figure 11 corresponds to the right plot in Figure 8 at a longshore distance of 33 yd. Given the level of dependency the shoreline position has on the tide, a simple linear regression used to identify trends of erosion or accretion is misleading and can result in falsified results.

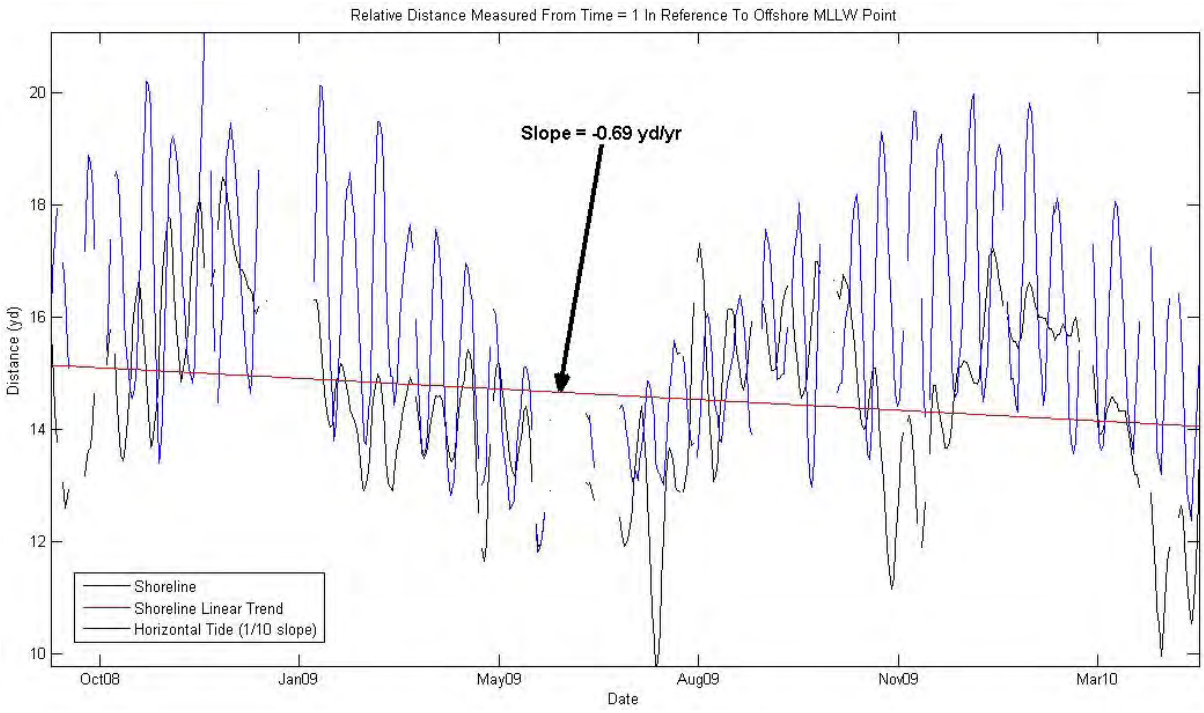

Figure 11 Transect 2 time series of shoreline position and tide at common reference

Taking advantage of the previous assumption that defines a common reference point for the shoreline and tide on day 1, a method is presented to remove the influence of tides

$$\Delta_i = X_{M_i} \longrightarrow i = 1$$
$$\Delta_i = X_{M_i} - \left(X_{M_{i-1}} + \left(X_{tide_i} - X_{tide_{i-1}}\right)\right) \longrightarrow i \geq 2 \quad (3)$$

where Δ is the measure of erosion or accretion, X_M is the observed shoreline position, X_{tide} is the horizontal tide component, and *i* is the time index. In theory, if the beach experienced no erosion or accretion the following day, the change in tide would define the new shoreline position. The difference between the theoretical and observed shoreline position is thus defined as erosion or accretion.

Results

Beach Response

Figure 12 shows the results of the shoreline change rate as described by equation 3. The 2-D plot shows both the temporal and spatial structure of the erosion (red) and accretion (blue) patterns. The plot to the right along the y-axis shows the mean transport rates as a function of longshore direction. The beach as a whole shows that over the study period it is accreting. The eastern region shows rates of accretion higher than in the western region. The plot on the bottom along the x-axis shows the transport rates integrated in the longshore direction as a function of time. The integration gives a measure of the surface planform of the beach, which is proportional to the volume given the previous assumption of a constant beach slope.

The plot in the bottom right corner shows the probability density of the sediment transport rates derived from changes in surface planform of the beach. The distribution can be described as Gaussian with a mean value equal to the overall beach accretion rate of 1885 yd^2/yr.

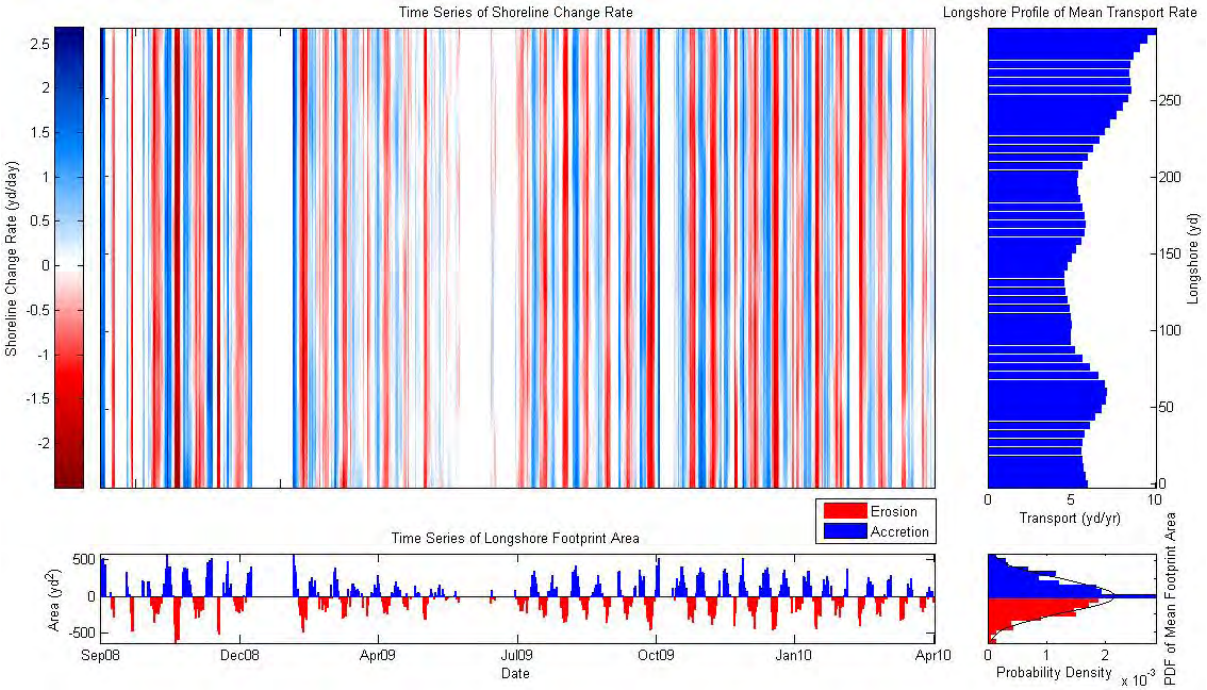

Figure 12 Top Left: 2-D shoreline change rate. **Top Right**: Profile of mean transport. **Bottom Left:** Time series of area change. **Bottom Right:** Histogram corresponding to time series of area change.

The cumulative change in the surface planform of the beach is shown in Figure 13. From a low frequency perspective, it is observed that the beach accretes from the beginning of the study period up to about January 2009. The beach then experiences a period of erosion up until about October 2009, followed by another period of accretion up until about February 2010. From there it undergoes erosion for the remainder of the study period. Figure 14 shows the trend of change rates as a function of longshore direction. This can be interpreted as a measure of stability for the identified accretion pattern. A negative trend indicates that the accretion pattern is decelerating over the study period.

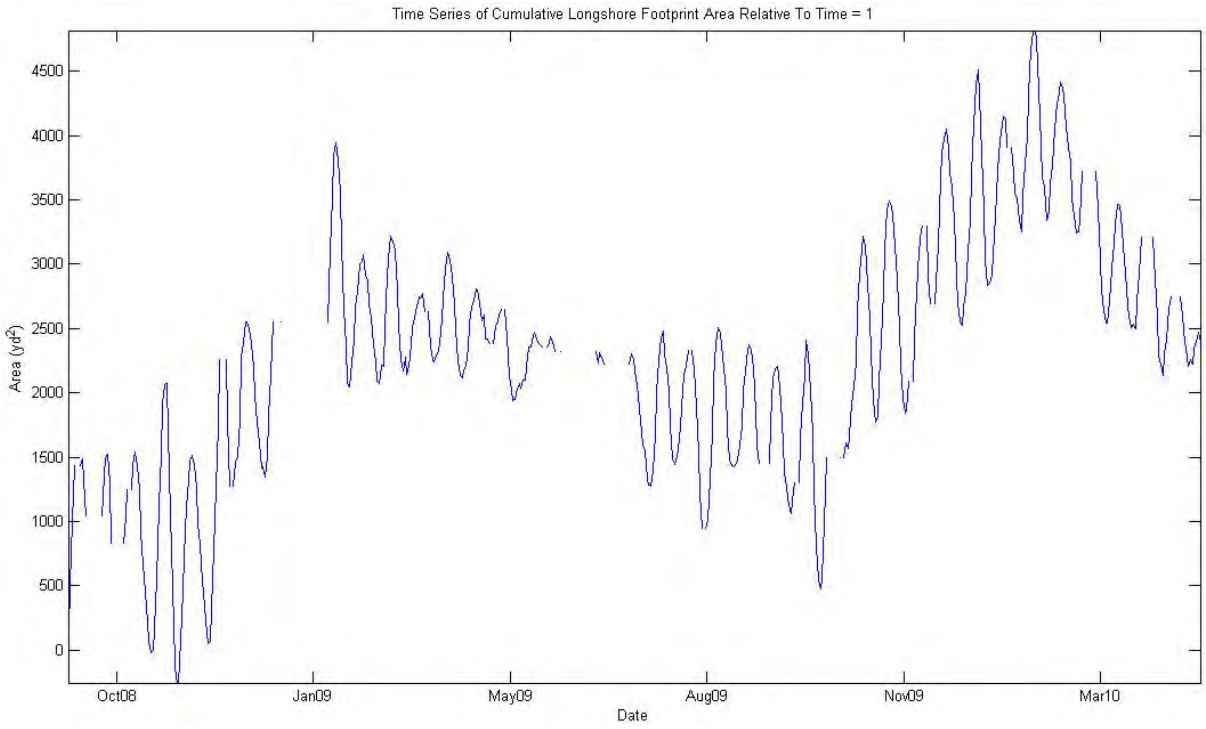

Figure 13 Cumulative time series of change in the surface planform of the beach

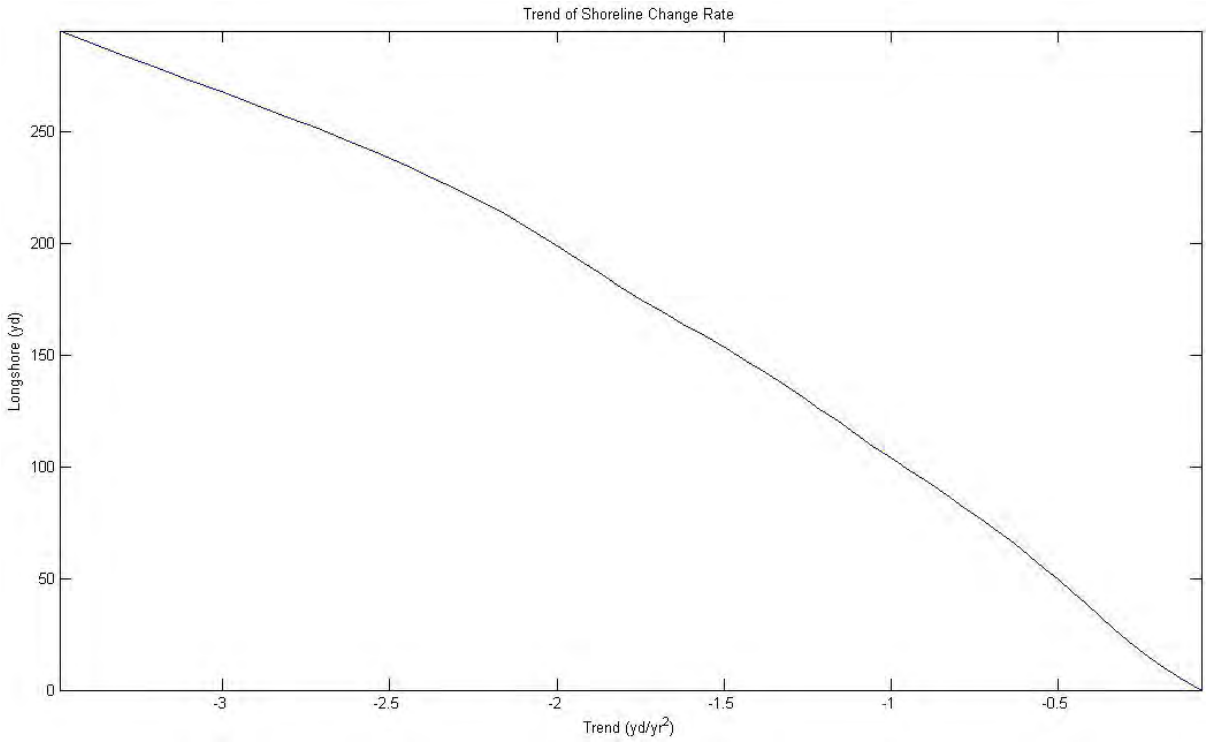

Figure 14 Trend of shoreline change rate

Forcing Parameters

With shoreline patterns identified, attention is turned to forcing parameters driving shoreline change. Figure 15 shows an overlay of the cumulative time series of change in the surface planform of the beach with the offshore parametric wave data. The results show no definitive correlation to the offshore wave data.

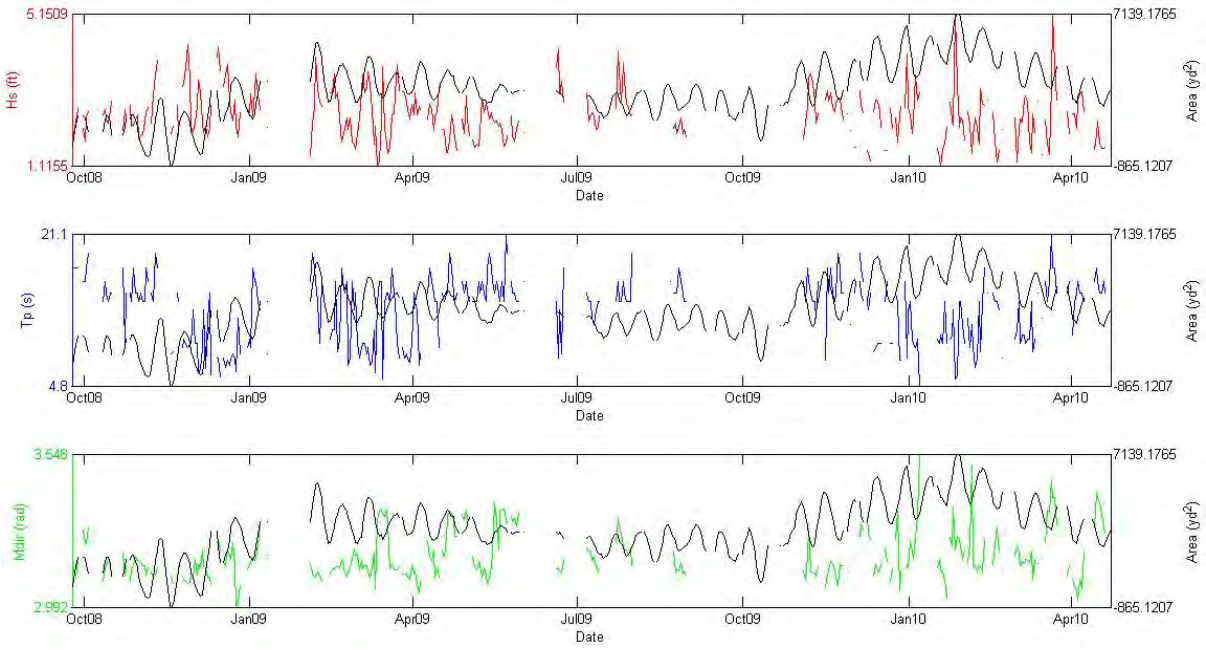

Figure 15 Kilo Nalu wave observations of significant wave height, peak period, and mean direction overlaid on cumulative time series of change in the surface planform of the beach (Figure 13). Note: the different scales.

To further investigate the nearshore wave field, case studies were conducted using a numerical wave model, Simulating WAves Nearshore (SWAN) (Booij et al., 1999). The boundary conditions were chosen based on the distributions of wave parameters over the study period shown in Figure 9. Each case study was simulated with a constant wave height of 3.28ft and direction of 180 degrees placing emphasis on evaluating the influence of wave period. Figure 16 shows the study site under each condition respectively, where white is land and the color represents significant wave height. In the case with a period of 14 s, it is shown that a greater amount of energy is present in the nearshore environment than with 8 s.

The spatial structure of the wave field is also significant. In each simulation, a dark blue region in the center of each image appears to attenuate the wave energy despite offshore wave conditions. Comparing the location of this region to Figure 4 shows that it is the reef hardground located offshore of the beach. The impact of the reef was examined periodically throughout the study period as shown in Figure 17. The nearshore portion of reef identified in the numerical simulation appears to remain constant though out the time series. The spatial and temporal variability of sediment transport over the reef elsewhere is apparent. Color coded bubbles aid in

identifying key features in the following discussion, but spatial and temporal patterns are not confined to the identified regions.

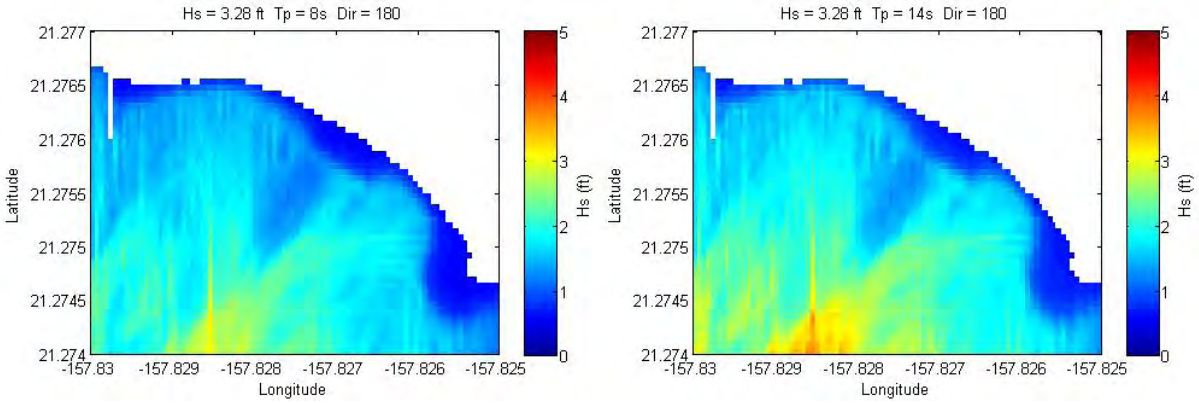

Figure 16 SWAN results from parametric case study based on wave observations **Left:** Hs = 3.28ft Tp = 8s Dir = 180deg. **Right:** Hs = 3.28ft Tp = 14s Dir = 180deg.

In Figure 17, red bubbles reveal an interesting feature in the field of view. Starting in October 2008, the reef flat is generally free of sand cover. By July 2009, a plume of sand is seen bisecting the reef flat starting from the eastern portion of the study site and continuing offshore in a westerly direction. It is unclear if the sand is moving offshore or onshore. In April 2009, the plume is no longer present, suggesting that this is a seasonal pattern.

Orange bubbles display a similar pattern to red ones, showing changes in the pattern of sand over the reef flat. Yellow and blue bubbles show temporal variability of the reef in the near field of view. In February 2009, the reef flat is free of sand while in February 2010, the reef flat appears mostly covered with sand. Referring to Figure 12, in February 2009 the beach appears to still be in an accretionary state, where as in February 2010 the beach appears to be in an erosive state. *This would imply that during an erosive state, sediment leaves the beach face and is transported offshore, covering the reef flat.*

Throughout most of the images, a brownish tint is seen in the water near the location of the blue bubbles. This is likely entrained sediment actively flowing within the water column. Following the arguments made in the case of the yellow bubbles, July 2009 is an erosive beach state and shows the reef in the near field of view covered with sand due to sediment transport from the beach face in the offshore direction. At the same time, the brownish tint in the water previously described is evident. *It is possible that a rip current is present, carrying sand off the beach face and subsequently covering the reef flat.* The same argument could be made for the sand plume in the red bubble described previously for July 2009. Such an assumption would indicate that *a sediment source/sink (temporary storage site) is located to the right central portion of the field of view.*

Oct 2008

Dec 2008

Feb 2009

Apr 2009

Jul 2009

Oct 2009

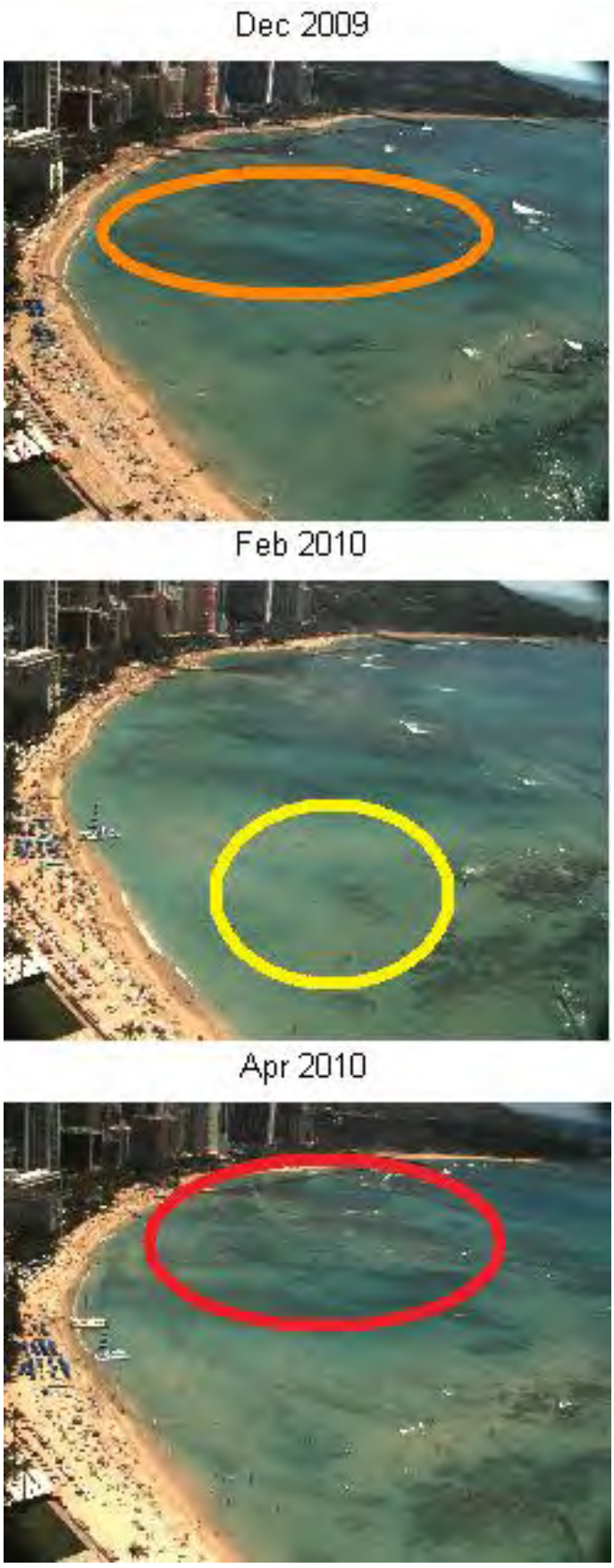

Figure 17 Sediment transport observations showing spatial and temporal variability

Discussion

Video imaging significantly improves the frequency of observations on shoreline position and allows for a detailed analysis of beach response. Studies of hydrodynamic and morphodynamic variability can be conducted on the same temporal and spatial scales. Shoreline detection by means of the CCD method has proven to be effective for the given conditions. The objective nature of the method does require a certain level of filtering though, primarily due to the high volume of traffic found in Waikiki.

In a traditional sense, applying a linear regression to the shoreline position alone, in order to define trends of erosion or accretion, can result in erroneous definitions. In the current study, a linear regression of the form Y=mX+b is not used for two main reasons. The first is due to the temporal scale of the study and the periodic nature of the shoreline position to accrete then erode. Consider a linear regression of the form Y=mX+b applied to a sine curve with a period (T) ranging from a 0.5T to 1.5T. The result will be highly dependent on the period over which the linear regression is conducted. The second reason is that the shoreline position is defined by equation (2) and is dependent on the hydrodynamic influences of local water levels at the beach face. For a given beach slope, vertical variations in the local water level translate to significant variations in the horizontal shoreline position. It is therefore imperative to remove tidal influences before defining beach erosion or accretion. The effects are portrayed in the comparison of erosion/accretion rates in Figure 8 and Figure 12. Figure 8 indicates rates of accretion less than those defined in Figure 12. Figure 8 also indicates that sections of the beach are eroding, while in Figure 12, the corresponding locations indicate that the beach is accreting. The methodology used in the current study results in the erosion/accretion rates presented in Table 1 below.

Table 1 – Rates of net shoreline change September 2008 to April 2010, Waikiki

Transect	Rate of change (yd/yr)
1	5.935645
2	5.748563
3	6.912597
4	4.912282
5	4.503962
6	5.712483
7	5.270532
8	6.957548
9	8.467028
10	10.01765

In this study, equation (2) is simplified due to the uncertainty associated with the temporal and spatial complexity generated by reef hardground and the limited availability of offshore wave observations. While tides play a dominate role in the variability of local water levels, the effects of wave setup and swash height should not be overlooked.

Comparing the cumulative time series of change in the surface planform of the beach to the offshore wave parameters, shown in Figure 15, reveals that some of the peaks and troughs in each time series correlate. By reducing equation (2) to be a function of tides only, it is expected that in some cases the wave parameters do correlate with the shoreline position, simply because of the dependency of shoreline position on wave setup and swash height, which are both dependent on incident conditions. It is for this reason that the results should be used with caution and it is important to not misinterpret the correlation as a cause and effect relationship. Again, small changes in the vertical, translate to significant changes in the horizontal for a given beach slope.

The beach slope is also assumed to be linear and constant over time in the present study. While this offers a valid estimation of the overall processes, the slope is actually a function of time and changes in response to the hydrodynamic forcing. As a means to investigate the influence of a variable linear slope, the present study was conducted under a variety of beach slopes. Evaluating profile surveys conducted by the University of Hawaii Coastal Geology Group, the beach slope in the current study is assumed to range between inverse slope values of 8-12. Figure 18 shows the relationship between beach slope and the rate of change in surface planform of the beach and indicates that the differences in the rate of change are insignificant given the scale of the study area.

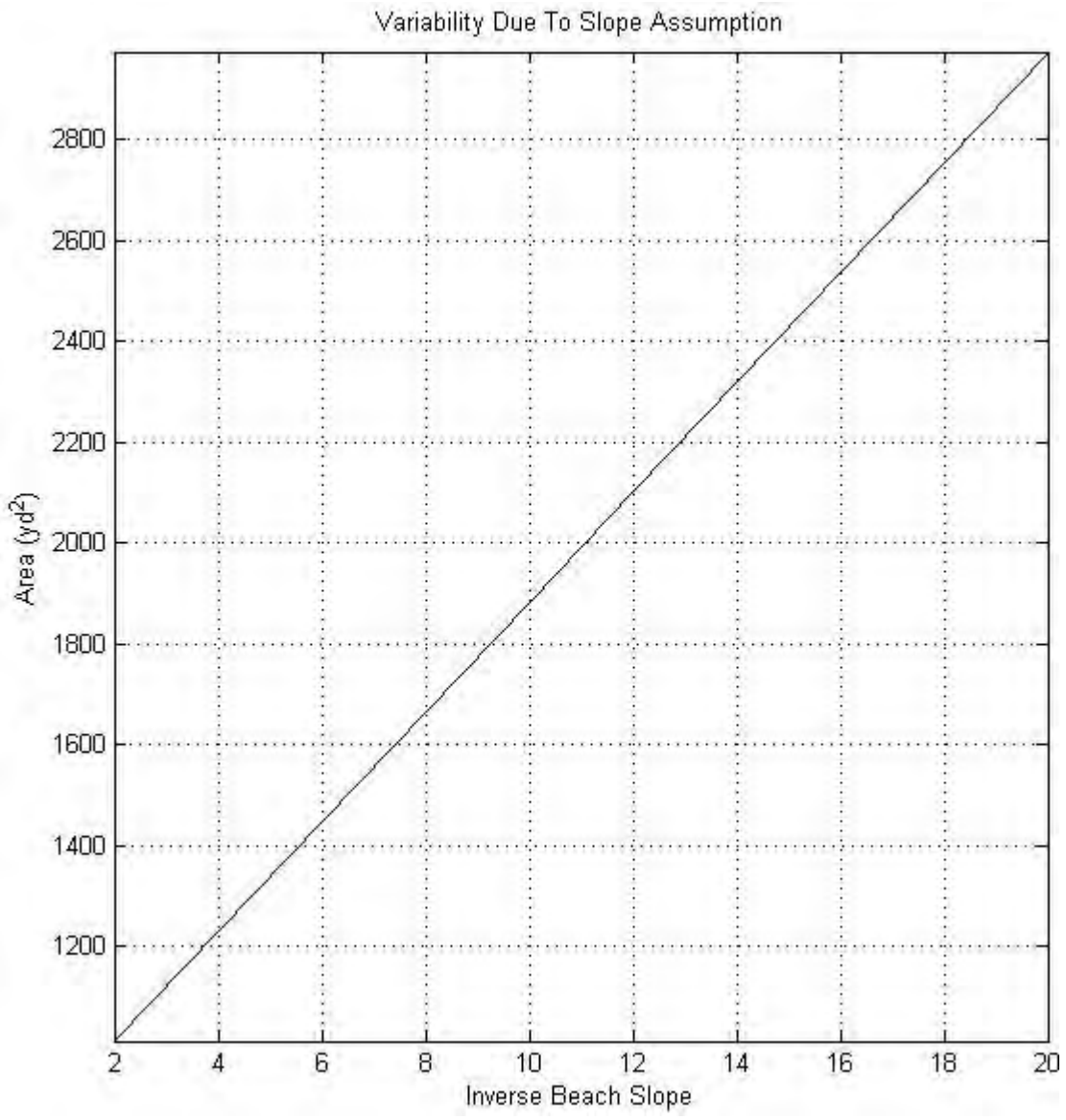

Figure 18 Rate of change in surface planform of the beach as a function of beach slope

The cumulative time series of change in the surface planform of the beach shown in Figure 13 appears to be somewhat periodic. The initial state of the beach is defined toward the end of the summer season and is erosive. It then undergoes a period of accretion throughout the beginning of the winter season. The cycle is not exactly seasonal, as it is dependent on the wave climate, which varies to some extent. The period of the study appears to cover one and a half cycles of the periodic pattern, displaying two seasons of accretion and one season of erosion. This would explain the apparent long-term trend of accretion in the time series. The onset of a new erosive season is seen towards the end of the study period with a slope that exceeds the previous season of erosion. This may indicate that the main erosive season displayed in the middle of the study period was rather mild and that the beach could experience more erosion in the year that follows.

Referring to the comparison between the cumulative time series of change in the surface planform of the beach and the offshore wave parameters, shown in Figure

15, it is clear that much of the wave data is missing during the summer months. While this hinders any definitive conclusions, it is believed that the cause of erosion during the summer season is due to the frequency of long period, high energy south swell events. This is supported by the observation that sediment is eroded from the beach face during summer months and transported offshore by means of a rip current, covering nearby reef flats. During periods of accretion, the sediment is removed from the reef flat and transported back to the beach face. Each of these arguments is shown and supported in Figure 17 and agrees with the findings of Wang and Gerritsen, 1995.

Conclusion

Prior to the application of video imagery, the study of beach morphodynamics was largely hindered by the surveying frequency of the beach both spatially and temporally. The affects of aliasing limited understanding to large temporal scales of variability. Furthermore, defined shoreline positions taken over large temporal scales were often used as a primary indication of erosion or accretion trends.

With the increase in temporal resolution afforded by video imagery, the dependency of shoreline position on local water levels is more evident. Small changes in the vertical water level resulting from tides and incident waves translate to significant changes in the horizontal component on a given beach slope. The current study proposes a method to remove the influence of hydrodynamic effects based on an assumption that on day 1 of the study, the hydrodynamics define the shoreline position. While the effects of wave setup and swash motion are ignored as a result of complexity and lack of wave data, results show that by removing tidal effects, the shoreline change rates differ from analyzing the shoreline position alone.

Over the course of the study, the beach displays an average aerial rate of accretion equal to 1885 yd^2/yr. Alongshore shoreline behavior displays spatial variability with the eastern region showing average rates of accretion larger than the region to the west. Cumulative changes in the surface planform of the beach of the shoreline position appear to be periodic, showing signals of erosion in the summer and accretion otherwise. The resulting long-term trend of the shoreline indicates net accretion but this may be the result of the time series extending across two seasons of accretion and only one season of erosion. The onset of a heavy erosive season at the end of the study period is apparent and could change the net shoreline position significantly. The main cause of erosion during the summer appears to be related to the long period, high energy south swell events.

References

Aarninkhof, S.G.J., 2003. Nearshore bathymetry derived from video imagery, Delft University of Technology, The Netherlands, PhD thesis, 175p.

Booij, N., Ris, R.C., Holthuijsen, L.H.., 1999. A third-generation wave model for coastal regions. J. Geophys. Res. 104, 7649-7666.

Campbell, F.J., 1972. Erosion and accretion of selected Hawaiian beaches. Report No. UNIHI-SEAGRANT-TR-72-02, University of Hawaii Sea Grant College Program, Honolulu, Hawaii.

Dail, H.J., Merrifield, M.A., Bevis, M., 2000. Steep beach morphology changes due to energetic wave forcing. Mar. Geol. 162, 443-458.

Gerritsen, F., 1978. Beach and surf parameters in Hawaii. Report No. UNIHI-SEAGRANT-TR-78-02, University of Hawaii Sea Grant College Program, Honolulu, Hawaii.

Gibbs, A., Richmond, B., Fletcher, C., Hillman, K., 2001. Hawaii beach monitoring program. U.S. Geological Survey Open-File Report 01-308.

Gourlay, M.R., 1996. Wave set-up on coral reefs. 2. Set-up on reefs with various profiles. Coast Eng. 28, 17-55.

Moberly, R., Chamberlain, T., 1964. Hawaiian beach systems. Report No. 64-2, Hawaiian Institute of Geophysics, University of Hawaii, Honolulu, Hawaii.

Norcross, Z.M., Fletcher, C.H., Merrifield, M., 2002. Annual and interannual changes on a reef-fringed pocket beach: Kailua Bay, Hawaii. Mar. Geol. 190, 553-580.

Turner, I., Leyden, V., Symonds, G., McGrath, J., Jackson, A., Jancar, T., Aarninkhof, S.G.J., Elshoff, I.E., 2001. Comparison of observed and predicted coastline changes at the gold coast artificial (surfing) reef, Sydney, Australia. In: EDGE, B.E. (ed.), Proceedings of the International Conference on Coastal Engineering, Sydney.

Wang, N., Gerritsen, F., 1995. Nearshore Circulation and dredged material transport at Waikiki Beach. Coast Eng. 24, 315-341.